

Battery Cell Equalization via Megahertz Multiple-Receiver Wireless Power Transfer

Ming Liu, *Member, IEEE*, Minfan Fu, *Member, IEEE*, Yong Wang, *Member, IEEE*, Chengbin Ma, *Member, IEEE*

Abstract—This paper proposes a new battery cell voltage equalization approach using multiple-receiver wireless power transfer (WPT) working at megahertz (MHz). Compared with existing multi-windings transformer, the megahertz multiple-receiver WPT system is advantageous in terms of saved weight and space, ease of implementation, and improved safety. In this paper, the unique operating principle of the WPT-based equalization is first explained, through which equalization currents are naturally determined by the battery cell voltage distribution. The currents are also analytically derived. This facilitates the discussion on power amplifier (PA) design. Performance analysis is then provided to investigate the influences of system parameters on the efficiency and equalization ability of the proposed WPT-based equalization system, and thus guide following design and implementation. Considering the uncertainty in PA load due to the random cell voltage distribution, a current-mode Class *E* PA is designed that enables approximately constant PA output current. Experimental results show that the proposed multiple-receiver WPT-based battery cell equalization system can achieve high overall system efficiency (above 71%) when equalizing six lithium-ion battery cells under loosely coupling ($k=0.065$). A good match between the experimental and calculation results also validates the correctness of the theoretical discussion.

I. INTRODUCTION

Lithium-ion batteries are now widely used energy storage devices in various applications such as electric vehicles and consumer electronic products thanks to their high energy density and power density [1]. In real applications, individual battery cells are usually connected to form a battery pack in order to provide high output voltage and high power capacity. Those cells inevitably have slightly different chemical and electrical characteristics. Thus after repeated charge and discharge, charge imbalance may occur in the form of unequal cell voltages. This eventually leads to shorter life-cycle and lower total capacity of the lithium-ion batteries [2], [3]. For a

lithium-ion battery pack, it is important to add a cell voltage equalization system for battery protection purposes [4].

Many battery cell voltage equalization schemes have been developed with different topologies and algorithms. They can be largely divided into two categories, passive and active approaches. In a passive equalization system, the cells with a higher voltage are discharged through resistors until all the cells reach the same cell voltage. Nowadays, most of battery packs, particularly in automotive applications, employ the passive equalization because it is straightforward to control and implement. Obviously, this passive approach has low energy efficiency because the excessive energy during equalization is simply dissipated. Potential temperature rise due to the generated heat may also cause other practical problems in design and implementation. Compared with the passive approaches, active equalization ones, such as using dc-dc converters and switched capacitor circuits, are promising to improve the energy efficiency during equalization [5]–[8]. At the same time, a large number of required switches complicate the design and lead to high cost and low reliability. In terms of reliability improvement, equalization using a multi-windings transformer is attractive. It uses less switches and thus potentially reduces the system complexity [9], [10]. However, in real applications, this solution suffers from problems such as added weight and difficulty in fabrication, particularly when the number of battery cells is large [11], [12].

In recent years, wireless power transfer (WPT) through inductive resonance coupling has become increasingly popular due to the possibility of enabling convenient and safe non-contacting charging. Especially, WPT working at megahertz (MHz) is now being widely considered as a promising technology for mid-range transfer of a medium amount of power [13], [14]. It is because a higher operating frequency (such as 6.78 MHz and 13.56 MHz) is usually desirable for building a more compact and lighter WPT system with a longer transfer distance. In addition, the increased spatial freedom by having a higher operating frequency in the MHz band makes it easier to achieve simultaneous wireless charging of multiple devices. Comparing with the existing multi-windings transformer, the multiple-receiver MHz WPT is easier to implement without the need of iron core. This unique advantage is particularly useful in case there is a large number of cells in a battery pack. For example, the transmitting and receiving coils in the MHz WPT systems can be made using printed circuit boards (PCBs). Thus the multiple-receiver WPT-based battery cell equalization system could be much thinner and lighter than that using the multi-windings transformer. To take a specific example, the transmitting coil in the final prototype system,

© 2017 IEEE. Personal use of this material is permitted. Permission from IEEE must be obtained for all other uses, including reprinting/republishing this material for advertising or promotional purposes, collecting new collected works for resale or redistribution to servers or lists, or reuse of any copyrighted component of this work in other works.

Manuscript received February 2, 2017; revised April 30, 2017; accepted May 15, 2017. This work was supported by the Shanghai Natural Science Foundation under Grant 16ZR1416300.

M. Liu and C. Ma are with University of Michigan-Shanghai Jiao Tong University Joint Institute, Shanghai Jiao Tong University, 800 Dongchuan Road, Minhang, Shanghai 200240, P. R. China (e-mail: mikeliu@sjtu.edu.cn; chbma@sjtu.edu.cn).

M. Fu is with the Center for Power Electronics Systems, Virginia Polytechnic Institute and State University, Blacksburg, VA 24061, USA (e-mail: minfanfu@vt.edu).

Y. Wang is with Department of Electrical Engineering, Shanghai Jiao Tong University, 800 Dongchuan Road, Minhang, Shanghai 200240, P. R. China (email: wangyong75@sjtu.edu.cn).

section V, is 1.6 mm in thickness and weights 73 g. It is also possible to integrate an individual receiving coil with a battery cell, which may potentially improve the flexibility and modularity of the equalization system. Besides, the non-contacting power transfer between the transmitting side and receiving side achieves safer equalization. The iron core in the transformers is not necessary in the multiple-receiver MHz WPT systems. Thus the possible consequences of core damage (short circuit, overheating, etc.) are completely eliminated. This advantage could help to lower the cost and difficulty in both design and fabrication of the battery cell equalization systems, particularly when working in harsh environments (shock, vibration, etc.).

This paper, for the first time, proposes a multiple-receiver WPT-based battery cell voltage equalization system working at MHz. The operating principle of the proposed WPT-based equalization is discussed based on the analytically derived equalization current. System performance analysis is then conducted to investigate the influences of system parameters on the efficiency and equalization ability of the proposed system. This analysis is important to guide following system design and implementation. The design of a current mode Class E PA is also discussed and developed that makes the proposed equalization system robust against a varying PA load caused by the random distribution of cell voltages. The experimental results validate the functionality and operating principle of the proposed system, and the theoretical discussions. In experiments, the prototype WPT-based equalization system achieves high system efficiency above 71% under a loosely coupled coupling ($k=0.065$) and with six receiving coils and six rectifiers. Note that Ref. [15] proposes a selective WPT design using a resonator-coupled two-pole band pass filter model and a dynamic capacitor network. The design exclusively delivers power to only one designated receiver through separating the resonant frequencies of the receivers. As explained in the following sections, this paper develops a unique multiple-receiver WPT-based battery cell equalization mechanism, through which equalization currents are naturally determined by the cell voltage distribution. The proposed scheme does not require active control and corresponding hardware and design. And different amounts of power are simultaneously transferred to the respective receivers with the same resonant frequency, i.e., 6.78 MHz here.

II. OPERATING PRINCIPLE

A. Circuit Configuration

Fig. 1 shows the circuit configuration of proposed multiple-receiver WPT-based battery cell voltage equalization system. As discussed in the introduction, it is a unique advantage of the MHz WPT systems, such as ones working at 6.78 MHz, to achieve simultaneous one-to-multiple wireless charging of battery cells. A current-mode Class E PA is introduced and designed due to 1) its high efficiency when operating at MHz, and 2) almost constant output current under a varying load. This PA consists of a classical Class E PA and an impedance transformation network, as shown in the figure. The classical Class E PA includes a switch Q , dc filter inductor

L_{dc} , series connected L_0 - C_0 matching network, and shunt capacitor C_s . The inductor L_{dc} should be sufficiently large such that only dc current can flow through it. Impedance Z_0 is the input impedance seen by the classical Class E PA. The impedance transformation network is further added to achieve approximately constant output current of the PA when PA load varies, i.e., different combination of states of cells, as discussed in section IV. This network consists of one series inductor L_{it} and two parallel capacitors $C_{it,l}$ and $C_{it,r}$.

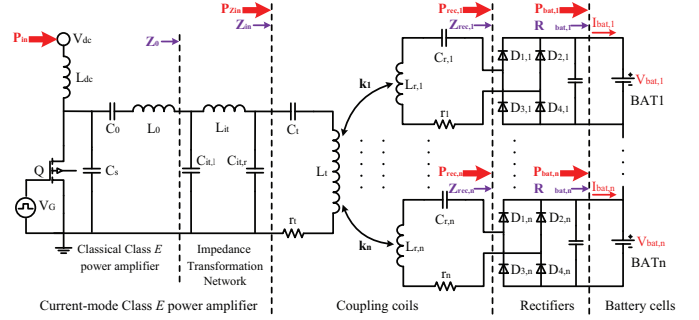


Fig. 1. Circuit configuration of the proposed WPT-based battery cell voltage equalization system.

In the above system, coupling coils are key components to transfer the charging power for cell equalization in a non-contacting manner. There are one transmitting coil and multiple receiving coils. L_t , C_t , and r_t are the self-inductance, compensation capacitor, and equivalent series resistance (ESR) of the transmitting coil, respectively. Similarly, $L_{r,i}$, $C_{r,i}$, and r_i ($i = 1, \dots, n$) are the self-inductance, compensation capacitor, and ESR of the i -th receiving coil, respectively. k_i is the mutual inductance coefficient between the transmitting coil L_t and i -th receiving coil. Note that in this specific application, all the receiving coils and their couplings with the transmitting coil, i.e., k_i 's, are expected to be identical.

In Fig. 1, P_{in} and $P_{Z_{in}}$ are the input power and output power of the current-mode Class E PA. $P_{rec,i}$ is the output power of the i -th receiving coil. $P_{bat,i}$ is the output power of the i -th rectifier. Z_{in} is the input impedance of the coupling coils seen by the PA, and $Z_{rec,i}$ is the input impedance of the i -th rectifier. $V_{bat,i}$ and $I_{bat,i}$ are the voltage and equalization current of the i -th battery cell. $R_{bat,i}$ is the i -th cell equivalent resistance. Note that fundamentally different with the existing equalization using the multi-windings transformer, the receiving coils in the proposed WPT-based equalization system can not provide a constant output voltage under different input impedances of the rectifiers, $Z_{rec,i}$. Detailed discussions on its unique operating principle and performance analysis are given as follows.

More specifically, in the existing voltage equalization systems using the multi-windings transformer, the output voltages of the secondary windings are solely determined by the turning ratio between the primary winding and secondary winding and the input voltage of the transformer. Thus it is straightforward to achieve equal and constant output voltages despite the varying input impedances of the rectifiers due to the different

cell voltages. The battery cell equalization current is simply determined by the cell voltage and leakage inductance of the transformer's secondary windings. On the other hand, the output voltages of the receiving coils in the proposed WPT-based equalization system, $V_{rec,i}$, depend on the values of the rectifier input impedance, mutual inductance coefficients, and PA output current. Thus, different with the existing solution using the multi-windings transformer, a comprehensive system-level analysis is important to explain the operating principle of the proposed multiple-receiver WPT-based equalization system.

B. Analytical Derivations

Fig. 2(a) shows the equivalent circuit of the proposed WPT-based battery cell voltage equalization system, in which the rectifiers are represented using their input impedances, $Z_{rec,i}$'s. Here L_r , C_r , and r are the self-inductance, compensation capacitor, and ESR of the identical receiving coils. Again, k is the identical mutual inductance coefficient between each receiving coil and the transmitting coil. $i_{Z_{in}}$ is the sinusoidal output current of the PA. From [16], the circuit model given in Fig. 2(a) is equivalent to a circuit shown in Fig. 2(b), in which all the receiving coils and their corresponding rectifier input impedances, $Z_{rec,i}$'s, are represented by reflected impedances, $Z_{in,i}$'s,

$$Z_{in,i} = R_{in,i} + jX_{in,i}, \quad (1)$$

where

$$R_{in,i} = \frac{\omega^2 k^2 L_t L_r (R_{rec,i} + r)}{(R_{rec,i} + r)^2 + (\omega L_r - \frac{1}{\omega C_r} + X_{rec,i})^2}, \quad (2)$$

$$X_{in,i} = -\frac{\omega^2 k^2 L_t L_r (\omega L_r - \frac{1}{\omega C_r} + X_{rec,i})}{(R_{rec,i} + r)^2 + (\omega L_r - \frac{1}{\omega C_r} + X_{rec,i})^2}, \quad (3)$$

and ω is the operating frequency of the WPT system. $R_{rec,i}$ and $X_{rec,i}$ are the resistance and reactance of $Z_{rec,i}$, namely the input impedance of the i -th rectifier. Under the resonance, i.e.,

$$j\omega L_t + \frac{1}{j\omega C_t} = 0, \quad (4)$$

$$j\omega L_r + \frac{1}{j\omega C_r} + jX_{rec,i} = 0. \quad (5)$$

$Z_{in,i}$ can be simplified as

$$Z_{in,i} = \frac{\omega^2 k^2 L_t L_r}{R_{rec,i} + r}, \quad (6)$$

namely pure resistive. Thus the power transferred from the transmitting coil to the i -th receiving coil can be derived as

$$P_{Z_{in,i}} = \frac{I_{Z_{in}}^2}{2} Z_{in,i} = \frac{I_{Z_{in}}^2 \omega^2 k^2 L_t L_r}{2(R_{rec,i} + r)}, \quad (7)$$

where $I_{Z_{in}}$ is the amplitude of $i_{Z_{in}}$. Considering the power loss occurs on r , the ESR of a receiving coil, the output power of the i -th receiving coil, $P_{rec,i}$, can be expressed as

$$P_{rec,i} = P_{Z_{in,i}} \cdot \frac{R_{rec,i}}{R_{rec,i} + r} = \frac{I_{Z_{in}}^2 \omega^2 k^2 L_t L_r}{2(R_{rec,i} + r)} \cdot \frac{R_{rec,i}}{R_{rec,i} + r}. \quad (8)$$

Assuming the efficiency of the i -th rectifier is $\eta_{rec,i}$, the charging power for the i -th battery cell is

$$P_{bat,i} = \frac{I_{Z_{in}}^2 \omega^2 k^2 L_t L_r R_{rec,i}}{2(R_{rec,i} + r)^2} \eta_{rec,i}. \quad (9)$$

Thus the equalization current is

$$I_{bat,i} = \frac{I_{Z_{in}}^2 \omega^2 k^2 L_t L_r R_{rec,i} \eta_{rec,i}}{2(R_{rec,i}^2 + 2R_{rec,i}r + r^2)V_{bat,i}}. \quad (10)$$

Because r^2 is usually much smaller than $R_{rec,i}^2$ (about 0.008 times in the following final experiments), (10) can be further simplified as

$$I_{bat,i} = \frac{I_{Z_{in}}^2 \omega^2 k^2 L_t L_r \eta_{rec,i}}{2(R_{rec,i} + 2r)V_{bat,i}}. \quad (11)$$

Note that in the above equation, $R_{rec,i}$ and $\eta_{rec,i}$ change with different $V_{bat,i}$.

Fig. 3 shows the circuit model of the full-bridge rectifier used in the proposed WPT-based equalization system. The rectifying diodes are modeled by their forward voltage drops, V_d . The sinusoidal input current of the rectifier, $i_{rec,i}$, can be expressed as

$$i_{rec,i} = I_{rec,i} \sin(\omega t) = \frac{\pi}{2} I_{bat,i} \sin(\omega t), \quad (12)$$

where $I_{rec,i}$ is the amplitude of $i_{rec,i}$. Based on the circuit model, the power loss in the i -th rectifier is

$$P_{loss,i} = \frac{1}{\pi} \int_0^\pi 2i_{rec,i} V_d d\omega t = 2V_d I_{bat,i}, \quad (13)$$

and the efficiency of the rectifier is

$$\eta_{rec,i} = \frac{P_{bat,i}}{P_{bat,i} + P_{loss,i}} = \frac{V_{bat,i}}{V_{bat,i} + 2V_d}. \quad (14)$$

It is known that the resistance of the full-bridge rectifier can be expressed as

$$R_{rec,i} = \frac{8}{\pi^2} R_{bat,i} = \frac{8}{\pi^2} \frac{V_{bat,i}}{I_{bat,i}}. \quad (15)$$

Substituting (14)(15) into (11) gives

$$I_{bat,i} = \frac{I_{Z_{in}}^2 \omega^2 k^2 L_t L_r}{4r(V_{bat,i} + 2V_d)} - \frac{4}{\pi^2 r} V_{bat,i}. \quad (16)$$

From (16), it can be seen that in the proposed equalization scheme, a higher battery cell voltage, $V_{bat,i}$, naturally leads to a lower equalization current. At the same time, the amplitude of the PA output current, $I_{Z_{in}}$, should be sufficiently large in order to avoid an unwanted negative $I_{bat,i}$ in (16). Thus, the following relationship must be guaranteed,

$$I_{Z_{in}} > \frac{4}{\pi \omega k} \sqrt{\frac{(V_{bat,i} + 2V_d)V_{bat,i}}{L_t L_r}}. \quad (17)$$

This requirement prefers a current-mode Class E PA that always provides an output current, $i_{Z_{in}}$, satisfying (17) despite the varying $V_{bat,i}$'s. Section IV gives detailed discussions on the estimation of the variation range of PA load and design of the current-mode Class E PA. Note that the mutual inductance coefficient k varies with different coil relative positions. It can

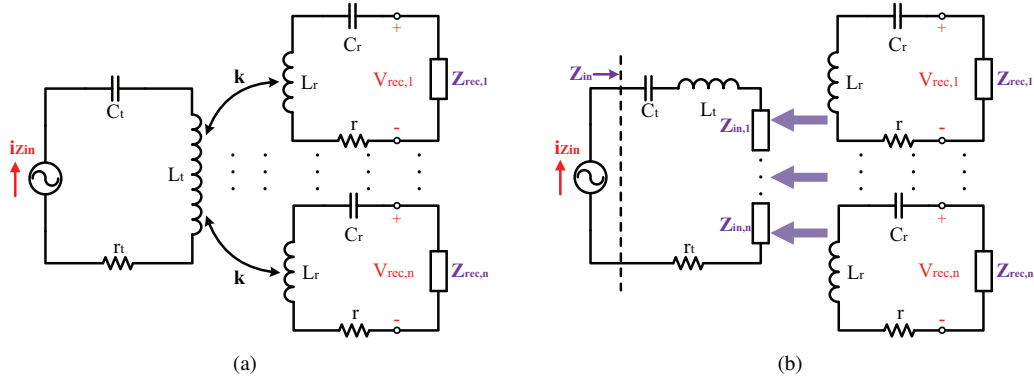


Fig. 2. Equivalent circuits of the WPT-based equalization system. (a) Equivalent circuit using Z_{rec} . (b) Equivalent circuit using Z_{in} .

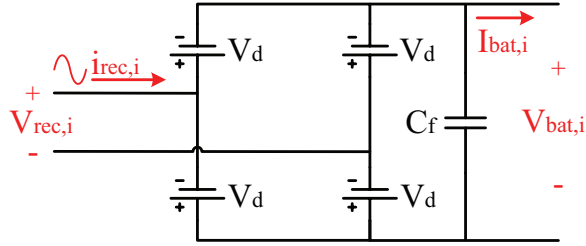


Fig. 3. Circuit model of the full-bridge rectifier.

be either measured or estimated in real applications [17], [18]. For the WPT-based cell equalization, the relative positions between the transmitting coil and receiving coils are usually fixed.

The operating principle of the proposed WPT-based battery cell voltage equalization is summarized as follows. Firstly, a higher/lower cell voltage leads to a higher/lower input resistance of the rectifier [refer to (15)]; Then, a specific receiving coil with a higher/lower input resistance of its rectifier obtains less/more power from the transmitting coil due to its lower/higher reflected impedance, namely the reversed relationship between the input resistance and reflected impedance explained by (6); Thus the rectifier delivers less/more power to the battery cell, which leads to a lower/higher equalization current [refer to (8)(11)]. Through this mechanism, the equalization currents are naturally determined by the distribution of the battery cell voltages.

From (12)(16), a lower battery cell voltage $V_{bat,i}$ leads to a higher charging current $I_{bat,i}$ and higher output current of the receiving coil (i.e., the input current of the rectifier $i_{rec,i}$). This results in a higher voltage across the receiving coil assuming identical inductances of receiving coils. Thus through the multiple-receiver WPT-based equalization the cell with a lower voltage naturally leads to a higher output voltage of its corresponding receiving coil, while the existing solution using the multi-windings transformer provides an equal output voltage of the secondary windings for all the cells. The proposed WPT-based equalization can potentially achieve a higher cell equalization ability. In addition, in the WPT-based equalization system, with an increasing number of cells the power loss on the receiving side increase. But power loss on the transmitting side is actually reduced due to the larger

total reflected resistance of the receivers [refer to Fig. 2 and (6)]. For the system using the multi-windings transformer, the power loss on the ESR of the primary winding arises due to the decreased input impedance of the transformer when the number of the cells increases. Thanks to the advantage of possible reduced power loss on the transmitting side, the proposed WPT-based equalization could yield a comparable efficiency level even with much weaker coupling of coils, particularly when the number of battery cells is large.

III. PERFORMANCE ANALYSIS

Based on the above discussion, the influences of system parameters over battery cell equalization ability and efficiency are analyzed as follows. The cell equalization ability, A_{equ} , is defined as

$$A_{equ} = \frac{I_{bat,j} - I_{bat,i}}{V_{bat,i} - V_{bat,j}} \text{ if } V_{bat,i} \neq V_{bat,j}, \quad (18)$$

where subscripts i and j represent the i -th and j -th battery cells, respectively. To achieve fast cell voltage equalization, it is expected that the difference in the equalization current (i.e., $I_{bat,j} - I_{bat,i}$) is as large as possible when the voltages of the two cells, $V_{bat,i}$ and $V_{bat,j}$, are not identical, namely a large A_{equ} . Substituting (16) into (18) gives

$$A_{equ} = \frac{I_{Zin}^2 \omega^2 k^2 L_t L_r}{4r(V_{bat,i} + 2V_d)(V_{bat,j} + 2V_d)} + \frac{4}{\pi^2 r}. \quad (19)$$

It can be seen that, besides the cell voltages, the system parameters also affect the equalization ability. As shown in (19), A_{equ} is proportional to product of inductances of the transmitting and receiving coils ($L_t L_r$), square of the operating frequency (ω), amplitude of the PA output current (I_{Zin}), and mutual inductance coefficient (k), while it is inversely proportional to the ESR of the receiving coils (r) and forward voltage drop of the rectifying diodes (V_d). Larger $L_t L_r$, ω , I_{Zin} , and k , similarly smaller r and V_d , help to improve the equalization ability. From Figs. 1 and 2, the overall equalization efficiency from the transmitting coil to rectifiers, $\eta_{coil2rec}$, is

$$\eta_{coil2rec} = \frac{\sum_{i=1}^n P_{bat,i}}{P_{Zin}} = \frac{\sum_{i=1}^n V_{bat,i} I_{bat,i}}{\frac{I_{Zin}^2}{2} \left(\sum_{i=1}^n Z_{in,i} + r_t \right)}. \quad (20)$$

Substituting (6)(15)(16) into (20) gives (21). The parameters, ω , k , L_t , and L_r , are largely pre-determined by the requirements from a specific application itself such as a target operating frequency in the ISM band (6.78 MHz here), required transfer distance, limitations on the available size and quality factor of the coupling coils. Thus instead of ω , k , L_t , and L_r , the values of A_{equ} and $\eta_{coil2rec}$ over various V_d , r , and $I_{Z_{in}}$ are calculated and shown in Fig. 4. A lithium-ion battery pack with six series connected cells is used as an example, and the nominal system parameters are listed in table I. The voltages of the six battery cells are assumed to be distributed as follows,

$$\begin{aligned} & [V_{bat,1}, V_{bat,2}, V_{bat,3}, V_{bat,4}, V_{bat,5}, V_{bat,6}] \\ & = [3.5, 3.6, 3.7, 3.8, 3.9, 4.0] \text{ (V)}. \end{aligned} \quad (22)$$

As shown in Fig. 4(a) and (b), higher diode forward voltage drop (V_d) and larger ESR of the receiving coil (r) result in lower equalization ability (A_{equ}) and efficiency ($\eta_{coil2rec}$). A_{equ} is more sensitive to the value of r , while V_d 's influence on $\eta_{coil2rec}$ is more obvious. Basically small r and V_d help to improve both the equalization ability and efficiency. Fig. 4(c) shows that the equalization ability improves with an increasing $I_{Z_{in}}$, which is consistent with the above analysis [refer to (19)]. However, the equalization efficiency, $\eta_{coil2rec}$, reaches its peak value at a specific $I_{Z_{in}}$, and then decreases if $I_{Z_{in}}$ further increases. This is due to the variations in $R_{rec,i}$ and $Z_{in,i}$ when $I_{Z_{in}}$ changes [refer to (2)(15)]. The PA output current should be properly chosen to simultaneously achieve high efficiency and meet the constraint in (17), i.e., its lower bound.

TABLE I
NOMINAL SYSTEM PARAMETERS.

$I_{Z_{in}}$	ω	k	V_d
1.5 A	6.78 MHz	0.065	0.3 V
L_t	r_t	L_r	r
4.27 μ H	1 Ω	0.46 μ H	0.35 Ω

In addition, according to (4)(5), ideally the compensation capacitors, C_t and C_r , should be designed to achieve full resonance between the transmitting and receiving coils taking into consideration the non-zero input reactance of the rectifiers, X_{rec} , at MHz [19]. Meanwhile, in the present specific application, due to the small equivalent resistances of the i -th battery cell (i.e., $R_{bat,i}$), $X_{rec,i}$ is small and neglectable when comparing with the reactance of the receiving coils. Thus here both C_t and C_r are directly determined to resonant with L_t and L_r , respectively, at the target operating frequency, 6.78 MHz.

IV. CURRENT-MODE CLASS E PA

The classical Class E PA is usually optimally designed, namely C_s and C_0 , targeting a single fixed load. However, in a practical battery cell equalization system, the random voltage distribution in the cells causes a varying load seen by the Class E PA, Z_{in} here. This makes the design of C_s and C_0 challenging. The varying Z_{in} may significantly affect

the efficiency and output current of the Class E PA, and thus leads to low system efficiency and undesired equalization current [refer to (16)]. For the present application, a high efficiency current-mode Class E PA, i.e., with approximately constant PA output current, is preferred. According to [20], if the variation range of the PA load, Z_{in} , is predictable, a high efficiency current-mode Class E PA can be achieved through an impedance transformation network and load-pull simulation in Advanced Design System (ADS), well-known radio frequency (RF) circuit simulation software from Keysight Technologies. In this paper, the design of the current-mode Class E PA is further developed for its specific application in battery cell equalization. First from (16), $R_{bat,i}$, the equivalent resistance of the i -th battery cell, can be expressed as

$$R_{bat,i} = \frac{V_{bat,i}}{I_{bat,i}} = \frac{32rV_{bat,i}(V_{bat,i} + 2V_d)}{\pi^2 I_{Z_{in}}^2 \omega^2 k^2 L_t L_r - 16V_{bat,i}(V_{bat,i} + 2V_d)}, \quad (23)$$

According to (6)(15)(23), it can be seen that a higher battery voltage $V_{bat,i}$ leads to a higher $R_{bat,i}$ and thus lower $Z_{in,i}$ and Z_{in} [refer to Fig. 2(b)]. Theoretically, the maximum and minimum values of Z_{in} , Z_{in}^{min} and Z_{in}^{max} , occur when all the battery cell voltages reach their upper or lower bounds, V_{bat}^{upper} and V_{bat}^{lower} . Again from (6)(15), the variation range of Z_{in} can be determined as

$$Z_{in} \in (Z_{in}^{min}, Z_{in}^{max}), \quad (24)$$

where

$$Z_{in}^{min} = \frac{n\pi^2 \omega^2 k^2 L_t L_r}{\frac{32n\pi^2 r V_{bat}^{upper}(V_{bat}^{upper} + 2V_d)}{\pi^2 I_{Z_{in}}^2 \omega^2 k^2 L_t L_r - 16V_{bat}^{upper}(V_{bat}^{upper} + 2V_d)} + \pi^2 r} + r_t, \quad (25)$$

and

$$Z_{in}^{max} = \frac{n\pi^2 \omega^2 k^2 L_t L_r}{\frac{32n\pi^2 r V_{bat}^{lower}(V_{bat}^{lower} + 2V_d)}{\pi^2 I_{Z_{in}}^2 \omega^2 k^2 L_t L_r - 16V_{bat}^{lower}(V_{bat}^{lower} + 2V_d)} + \pi^2 r} + r_t. \quad (26)$$

The upper and lower bounds of the voltage of example battery cell in the following final experiments, SANYO UR18650A, are 3.5 V and 4.2 V, respectively. With the system parameters listed in Table I, the variation range of Z_{in} is derived as

$$Z_{in} \in (4.7 \Omega, 48 \Omega). \quad (27)$$

For a classical Class E PA, it is known that C_s and C_0 can be determined using the following equations, in which a fixed target load, Z_{in} , is assumed [21],

$$C_s = \frac{0.1836}{\omega Z_{in}}, \quad (28)$$

$$C_0 = \frac{1}{\omega^2 L_0 - 1.1525\omega Z_{in}}. \quad (29)$$

Here an intermediate Z_{in} ($=25 \Omega$) within the range in (27) is chosen as a target load. The design parameters, C_s and C_0 , are then calculated as 170 pF and 680 pF, respectively. Based on the circuit model of the classical Class E PA in Fig. 5(a) and parameters listed in Table II, the PA load-pull simulation is carried out and results are given in Fig. 5(b). Here $r_{L_{dc}}$ and r_{L_0} are the ESRs of the dc filter inductor L_{dc} and ac series

$$\eta_{coil2rec} = \frac{2 \sum_{i=1}^n \left[\frac{V_{bat,i} I_{Z_{in}}^2 \omega^2 k^2 L_t L_r}{4r(V_{bat,i} + 2V_d)} - \frac{4}{\pi^2 r} V_{bat,i}^2 \right]}{I_{Z_{in}}^2 \left\{ \sum_{i=1}^n \frac{\pi^2 \omega^2 k^2 L_t L_r [I_{Z_{in}}^2 \omega^2 k^2 L_t L_r \pi^2 r - 16r V_{bat,i} (V_{bat,i} + 2V_d)]}{16\pi^2 r^2 V_{bat,i} (V_{bat,i} + 2V_d) + I_{Z_{in}}^2 \omega^2 k^2 L_t L_r \pi^2 r} + r_t \right\}}. \quad (21)$$

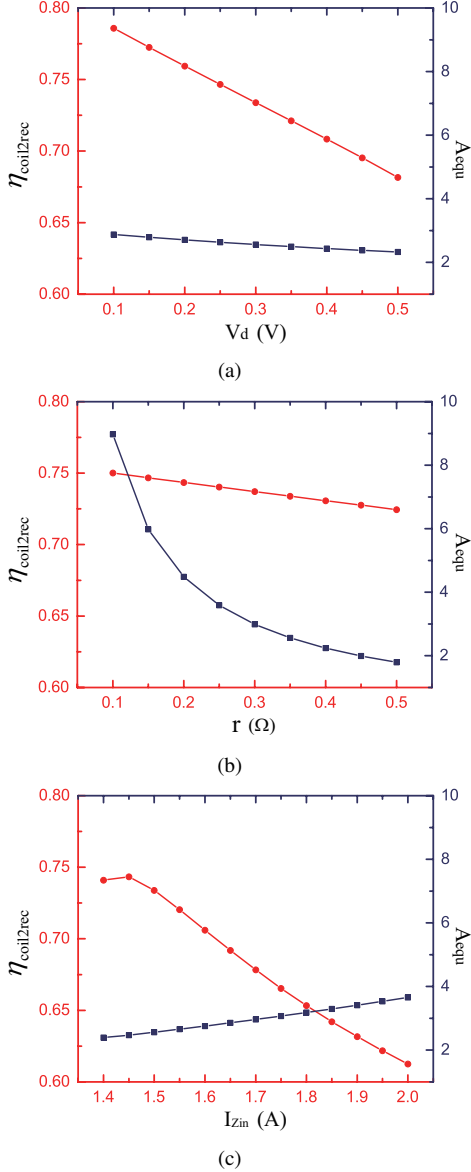


Fig. 4. Equalization ability (A_{equ}) and efficiency ($\eta_{coil2rec}$) over various parameters. (a) V_d . (b) r . (c) $I_{Z_{in}}$.

inductor L_0 , respectively. In Fig. 5(b), i.e., the Smith chart, the blue contours are for the constant output power, and the red contours show constant PA efficiencies. The two contours provide an overview of the PA performance under the different loads [20]. The brown dash line represents the varying load Z_{in} from 4.7 to 48 Ω [refer to (27)]. It goes through the high PA efficiency region and extends to the low efficiency one [refer to red contours]. Meanwhile, with the increasing Z_{in} , the PA output power ($\frac{I_{Z_{in}}^2 Z_{in}}{2}$), i.e., blue contours, does

not increase proportionally, which indicates decreasing PA output current. As shown in Fig. 5(b), for an efficient operation of the Class E PA, it is preferred that the PA load varies within the high efficiency region, which is represented by the red contours in the figure. With the properly tuned impedance transformation network (i.e., $C_{it,l}$ and $C_{it,r}$) in Fig. 1, the trajectory of the PA load can be approximately transformed from the brown dash line Z_{in} to the green target line Z_0 . The new trajectory of Z_0 locates in the high efficiency region and is almost perpendicular to the power contours. Thus the output power of the PA proportionally increases with an increasing Z_0 . This enables close-to-constant output PA current. The target line of Z_0 is determined by the amplitude of $i_{Z_{in}}$ and variation range of Z_{in} . Assuming the amplitude of $i_{Z_{in}}$ is chosen as 1.5 A (as same as in the final experiments), the target range of the PA output power at the lower and upper bounds of Z_{in} , 4.7 Ω and 48 Ω , is between 5.3 W and 54 W. Z_0 should also vary within the high efficiency range. The final designs of $C_{it,l}$ and $C_{it,r}$ are listed in Table II.

TABLE II
PARAMETERS OF CLASS E PA AND IMPEDANCE TRANSFORMATION NETWORK.

V_{dc}	L_{dc}	$r_{L_{dc}}$	L_0	r_{L_0}
35 V	12 μ H	0.1 Ω	1.465 μ H	0.2 Ω
C_s	C_0	L_{it}	$C_{it,l}$	$C_{it,r}$
170 pF	680 pF	330 nH	330 pF	390 pF

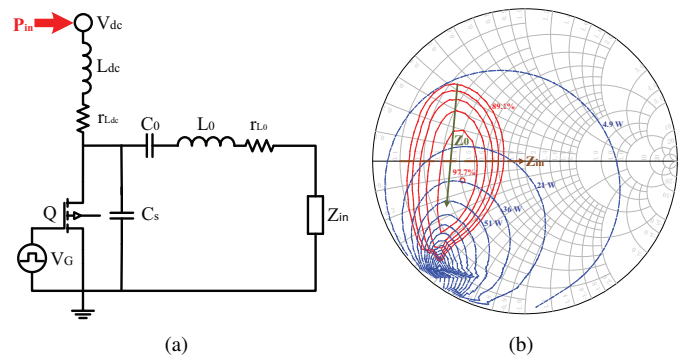


Fig. 5. Load-pull simulation of the classical Class E PA. (a) Circuit model. (b) Results.

V. EXPERIMENTAL VERIFICATION

A prototype 6.78-MHz multiple-receiver WPT system is built up to verify the proposed concept of WPT-based battery cell equalization. The experimental setup is shown in Fig. 6. Its configuration is as same as that in Fig. 1, which includes a current-mode Class E PA, a transmitting coil, six receiving

coils, six rectifiers, and a lithium-ion battery pack (six SANYO UR18650A cells connected in series). All the six receiving coils and rectifiers are identical and implemented on the same printed circuit board (PCB). Note that during the design of the coupling coils, the trace thickness on PCB should be carefully selected as well as the shape, turns, trace width, and trace spacing of the coils to reduce the skin and proximity losses at a high operating frequency such as 6.78 MHz here. The trace thickness in the present prototype WPT system is $35\mu\text{m}$. Schottky diodes, DFSL240L, and MOSFET, SUD15N15, work as rectifying diodes and switch in Class E PA, respectively. The parameters listed in Tables I and II are applied in the experiments. The air gap between the transmitting coil and receiving coils are 30 mm ($k=0.065$). The compensation capacitors, C_t and $C_{r,i}$'s, are calculated to let the transmitting coil and receiving coils resonant at 6.78 MHz (130 pF and 1225 pF, respectively). The PA output current is chosen as 1.5 A that meets the requirement in (17).

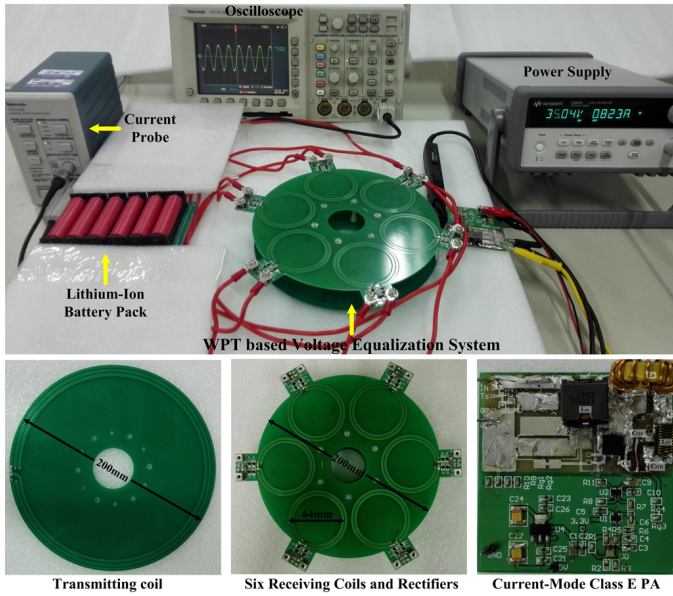


Fig. 6. The experimental setup of the prototype multiple-receiver WPT based battery equalization system.

Fig. 7 gives the voltages of the battery cells during the entire equalization process. The initial voltages of the cells are different emulating a realistic case that requires the cell equalization. It can be seen that all the cell voltages naturally converge to the same level without any active control of the input voltage and current. In this specific experiment and setup of the system, the voltage differences among the cells are less than 50 mV after about 110 mins.

Fig. 8 shows the output current of the designed current-model Class E PA. The PA output current is almost constant around the target value, 1.5 A, with the varying battery cell voltages in Fig. 7. This experimental result validates the derivations of variation range of Z_{in} and design of the current-mode Class E PA. The theoretical lower bound of the required PA output current, the dash line, is also shown in this figure. The value, 1.47 A, is calculated by using (17) when $V_{bat,i} =$

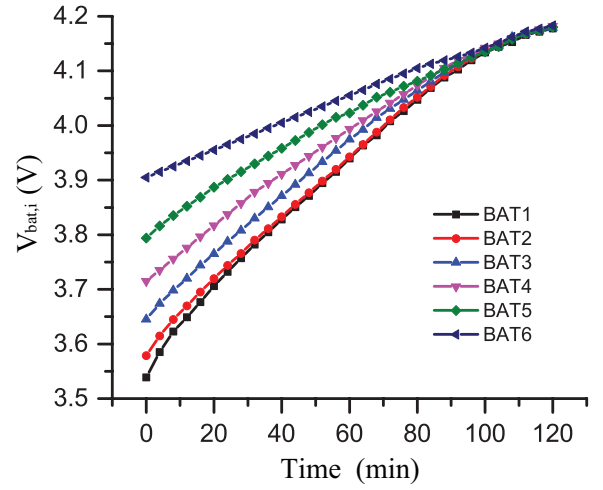


Fig. 7. Battery cell voltages in experiments.

4.2 V, i.e., the upper bound of the cell voltage. The actual PA output current satisfies the requirement in (17).

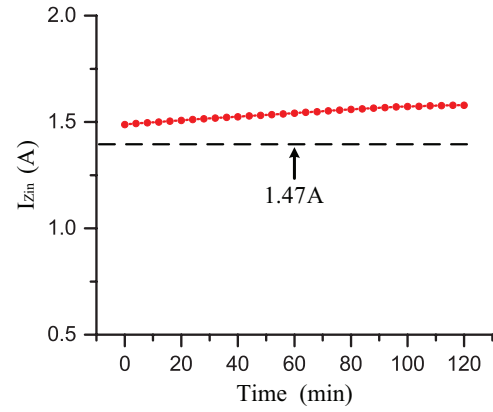


Fig. 8. Output current of the current-model Class E PA in experiments.

The cell equalization currents are shown in Fig. 9. Through the proposed WPT-based equalization, the cells with higher initial voltages are naturally charged with smaller currents. The calculated results are also shown for comparison purposes, which use (16) and the experimental results of $I_{Z_{in}}$ in Fig. 8. Again, a good match between the experimental (exp.) and calculation (cal.) results validates the operating principle discussed in section II-B. Generally, the battery cell equalization system is different with a battery charger. The purpose of the equalization system is to balance the cell voltages in a battery pack either during or after repeat charge and discharge. Usually for the charge of lithium-ion batteries, a specific profile such as the well-known Constant Current-Constant Voltage (CC-CV) profile needs to be strictly followed by the battery charger in order to avoid the deterioration of the cells.

The efficiency and output power of the prototype multiple-receiver WPT-based equalization system are given in Fig. 10. The increasing cell voltages during the equalization result in higher efficiencies of the receiving coils and rectifiers, and thus higher system efficiency [refer to (14)]. The overall

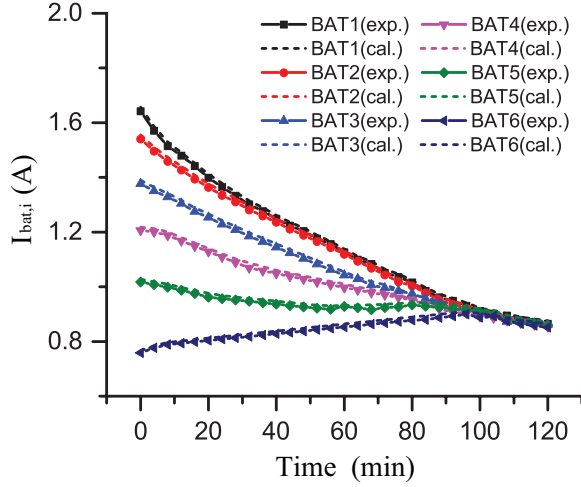


Fig. 9. Battery equalization currents in experiments.

equalization system achieves high system efficiency over 71% during the entire equalization process and, more importantly, with loosely coupled coils ($k=0.065$). On the contrary, the output power of the equalization system becomes lower with increased cell voltages. As shown in (25), higher cell voltages lead to lower input impedance of the coupling coils, Z_{in} . Meanwhile, the output current of the current-mode Class E PA is still almost constant, as shown in Fig. 8. Naturally both the input power of the coupling coils and thus output power of the overall system become lower during the equalization.

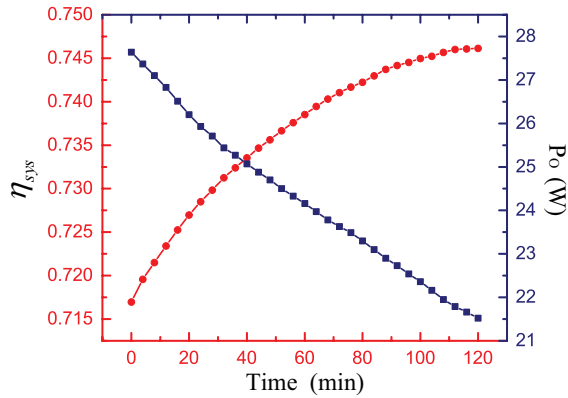


Fig. 10. System efficiency and output power in experiments.

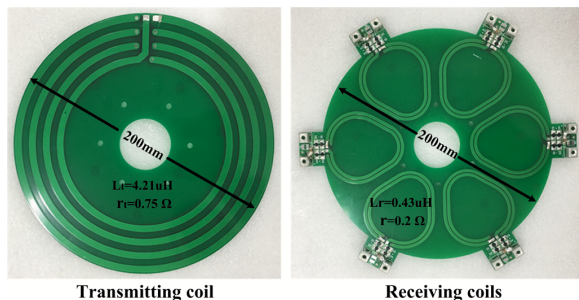


Fig. 11. Improved design of the coupling coils.

For reference purposes, the design of coupling coils (shape, turns, trace width, and trace spacing) is further optimized, as shown in Fig. 11. The parameters of the newly designed coils are given in the figure. With the same outer diameter, besides the reduced ESRs of the coils, the mutual inductance coefficient is also improved (0.067) under the same transfer distance. Table III compares the transmission efficiencies of the original and improved coupling coils under the same sets of example cell voltages, η_{coil} and η_{coil}^* . The transmission efficiency is defined as [see Fig. 1],

$$\eta_{coil} = \frac{\sum_{i=1}^6 P_{rec,i}}{P_{z_{in}}} \quad (30)$$

Due to the complicated multiple-receiver configuration, it is challenging to accurately measure the total ac output power of the six receivers. Here the efficiencies of the coupling coils are obtained based on the measured $\eta_{coil2rec}$ (the efficiency from transmitting coil to rectifiers defined in (20)) and the calculated rectifier efficiencies given in (14). It can be seen that the improved coupling coils can achieve a high transmission efficiency in the present application of battery cell voltage equalization, above 92%, namely a comparable efficiency to that of the multi-windings transformer.

TABLE III
TRANSMISSION EFFICIENCIES OF COUPLING COILS.

$V_{bat,1}$	$V_{bat,2}$	$V_{bat,3}$	$V_{bat,4}$	$V_{bat,5}$	$V_{bat,6}$	$\eta_{coil}/\eta_{coil}^*$
3.54 V	3.58 V	3.65 V	3.72 V	3.79 V	3.91 V	85.4/91.8%
3.71 V	3.72 V	3.77 V	3.82 V	3.89 V	3.96 V	86.4/92.3%
3.83 V	3.83 V	3.87 V	3.91 V	3.96 V	4.01 V	87.0/92.5%
3.94 V	3.94 V	3.98 V	3.99 V	4.02 V	4.06 V	87.5/92.6%
4.05 V	4.05 V	4.06 V	4.07 V	4.08 V	4.11 V	87.8/92.7%
4.18 V	88.2/92.8%					

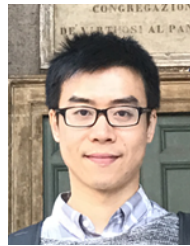
VI. CONCLUSIONS

In this paper, the MHz multiple-receiver WPT-based battery voltage equalization is proposed and investigated through both analytical derivations and experiments. Its operating principle, a natural equalization mechanism, and the requirement on the PA output current are first explained. The discussions on equalization ability and efficiency are then given that show the influences of the system parameters and guide the following design and implementation. In real applications, there is an uncertainty on the PA load due to the random cell voltage distribution. In order to maintain the efficiency and output current of the classical Class E PA, an impedance transformation network is added and designed to achieve a current-mode Class E PA. This PA provides approximately constant output current within the entire equalization process. Experimental results show that the prototype MHz multiple-receiver WPT-based equalization system achieves high system efficiency (above 71%) with loosely coupled coils ($k=0.065$) when equalizing six lithium-ion battery cells.

REFERENCES

- [1] A. Khaligh and Z. Li, "Battery, ultracapacitor, fuel cell, and hybrid energy storage systems for electric, hybrid electric, fuel cell, and plug-in hybrid electric vehicles: State of the art," *IEEE Trans. Veh. Technol.*, vol. 59, no. 6, pp. 2806–2814, Jul. 2010.

- [2] L. Maharjan, T. Yamagishi, and H. Akagi, "Active-power control of individual converter cells for a battery energy storage system based on a multilevel cascade PWM converter," *IEEE Trans. Power Electron.*, vol. 27, no. 3, pp. 1099–1107, Mar. 2012.
- [3] C. S. Lim, K. J. Lee, N. J. Ku, D. S. Hyun, and R. Y. Kim, "A modularized equalization method based on magnetizing energy for a series-connected lithium-ion battery string," *IEEE Trans. Power Electron.*, vol. 29, no. 4, pp. 1791–1799, Apr. 2014.
- [4] P. A. Cassani and S. S. Williamson, "Design, testing, and validation of a simplified control scheme for a novel plug-in hybrid electric vehicle battery cell equalizer," *IEEE Trans. Ind. Electron.*, vol. 57, no. 12, pp. 3956–3962, Dec. 2010.
- [5] M. Einhorn, W. Guertlschmid, T. Blochberger, R. Kumpusch, R. Permann, F. V. Conte, C. Kral, and J. Fleig, "A current equalization method for serially connected battery cells using a single power converter for each cell," *IEEE Trans. Veh. Technol.*, vol. 60, no. 9, pp. 4227–4237, Nov. 2011.
- [6] Y. Yuanmao, K. W. E. Cheng, and Y. P. B. Yeung, "Zero-current switching switched-capacitor zero-voltage-gap automatic equalization system for series battery string," *IEEE Trans. Power Electron.*, vol. 27, no. 7, pp. 3234–3242, Jul. 2012.
- [7] M. Uno and K. Tanaka, "Influence of high-frequency charge-discharge cycling induced by cell voltage equalizers on the life performance of lithium-ion cells," *IEEE Trans. Veh. Technol.*, vol. 60, no. 4, pp. 1505–1515, May 2011.
- [8] F. Mestrallet, L. Kerachev, J. C. Crebier, and A. Collet, "Multiphase interleaved converter for lithium battery active balancing," *IEEE Trans. Power Electron.*, vol. 29, no. 6, pp. 2874–2881, Jun. 2014.
- [9] N. H. Kutkut, D. M. Divan, and D. W. Novotny, "Charge equalization for series connected battery strings," *IEEE Trans. Ind. Appl.*, vol. 31, no. 3, pp. 562–568, May 1995.
- [10] A. Xu, S. Xie, and X. Liu, "Dynamic voltage equalization for series-connected ultracapacitors in EV/HEV applications," *IEEE Trans. Veh. Technol.*, vol. 58, no. 8, pp. 3981–3987, Oct. 2009.
- [11] H. S. Park, C. H. Kim, K. B. Park, G. W. Moon, and J. H. Lee, "Design of a charge equalizer based on battery modularization," *IEEE Trans. Veh. Technol.*, vol. 58, no. 7, pp. 3216–3223, Sep. 2009.
- [12] M. Uno and A. Kukita, "Single-switch single-transformer cell voltage equalizer based on forward-flyback resonant inverter and voltage multiplier for series-connected energy storage cells," *IEEE Trans. Veh. Technol.*, vol. 63, no. 9, pp. 4232–4247, Nov. 2014.
- [13] A. Kurs, A. Karalis, R. Moffatt, J. D. Joannopoulos, P. Fisher, and M. Soljačić, "Wireless power transfer via strongly coupled magnetic resonances," *Science*, vol. 317, no. 5834, pp. 83–86, Jul. 2007.
- [14] S. Hui, W. Zhong, and C. Lee, "A critical review of recent progress in mid-range wireless power transfer," *IEEE Trans. Power Electron.*, vol. 29, no. 9, pp. 4500–4511, Sep. 2014.
- [15] Y. J. Kim, D. Ha, W. J. Chappell, and P. P. Irazoqui, "Selective wireless power transfer for smart power distribution in a miniature-sized multiple-receiver system," *IEEE Trans. Ind. Electron.*, vol. 63, no. 3, pp. 1853–1862, Mar. 2016.
- [16] M. Fu, T. Zhang, C. Ma, and X. Zhu, "Efficiency and optimal loads analysis for multiple-receiver wireless power transfer systems," *Trans. Microw. Theory Tech.*, vol. 63, no. 3, pp. 801–812, Mar. 2015.
- [17] S. Nakamura, M. Namiki, Y. Sugimoto, and H. Hashimoto, "Q controllable antenna as a potential means for wide-area sensing and communication in wireless charging via coupled magnetic resonances," *IEEE Trans. Power Electron.*, vol. 32, no. 1, pp. 218–232, Jan. 2017.
- [18] S. Nakamura and H. Hashimoto, "Error characteristics of passive position sensing via coupled magnetic resonances assuming simultaneous realization with wireless charging," *IEEE Sensors J.*, vol. 15, no. 7, pp. 3675–3686, Jul. 2015.
- [19] M. Liu, M. Fu, and C. Ma, "Parameter design for a 6.78-MHz wireless power transfer system based on analytical derivation of class E current-driven rectifier," *IEEE Trans. Power Electron.*, vol. 31, no. 6, pp. 4280–4291, Jun. 2016.
- [20] S. Liu, M. Liu, S. Yang, C. Ma, and X. Zhu, "A novel design methodology for high-efficiency current-mode and voltage-mode class-E power amplifiers in wireless power transfer systems," *IEEE Trans. Power Electron.*, vol. 32, no. 6, pp. 4514–4523, Jun. 2017.
- [21] M. Albulet, *RF power amplifiers*. SciTech Publishing, 2001.



Ming Liu (S'15-M'17) received the B.S. degree from Sichuan University, Sichuan, China, in 2007, and the M.S. degree from the University of Science and Technology Beijing, Beijing, China, in 2011, both in mechatronic engineering. He is currently working toward the Ph.D. degree in electrical and computer engineering at University of Michigan-Shanghai Jiao Tong University Joint Institute, Shanghai Jiao Tong University, Shanghai, China.

His research interests include high frequency power electronic circuits such as high frequency resonant converters and megahertz wireless power transfer systems, general power electronics and applications, circuit-level and system-level optimization.



Minfan Fu (S'13-M'16) received the B.S., M.S., and Ph.D. degrees in electrical and computer engineering from University of Michigan-Shanghai Jiao Tong University Joint Institute, Shanghai Jiao Tong University, Shanghai, China in 2010, 2013, and 2016, respectively.

He is currently a postdoctoral researcher at the Center for Power Electronics Systems, Virginia Polytechnic Institute and State University, Blacksburg, VA, USA. His research interests include megahertz wireless power transfer, resonant converters,

and circuit design optimization.



Yong Wang (M'05) received his Ph.D. degree in power electronics from Zhejiang University in 2005. After receiving his Ph.D. degree, from 2005-2008, he was a senior researcher in Samsung Advanced Institute of Technology in Korea, researching on the fuel cell grid tied inverter. From 2008-2010, he was working in Danfoss, Denmark, as a power electronics hardware engineer. In 2010, he joined Shanghai Jiao Tong University, Shanghai, China.

Currently he is an associate professor in the Department of Electrical Engineering, Shanghai Jiao Tong University. His main research fields includes wireless charging transfer, multi-level conversion, etc.



Chengbin Ma (M'05) received the B.S. (Hons.) degree in industrial automation from East China University of Science and Technology, Shanghai, China, in 1997, and the M.S. and Ph.D. degrees in electrical engineering from The University of Tokyo, Tokyo, Japan, in 2001 and 2004, respectively.

He is currently an associate professor of electrical and computer engineering at University of Michigan-Shanghai Jiao Tong University Joint Institute, Shanghai Jiao Tong University, Shanghai, China. Between 2006 and 2008, he held a postdoctoral position with the Department of Mechanical and Aeronautical Engineering, University of California Davis, California, USA. From 2004 to 2006, he was a R&D researcher with Servo Laboratory, Fanuc Limited, Yamanashi, Japan. He is an associate editor of the IEEE Transactions on Industrial Informatics. His research interests include networked energy systems, wireless power transfer, and mechatronic control.